

# Detection and removal of clutter and anaprop in radar data using a statistical scheme based on echo fluctuation

J. Sugier<sup>1</sup>, J. Parent du Châtelet<sup>2</sup>, P. Roquain<sup>2</sup>, and A. Smith<sup>1</sup>

<sup>1</sup>Radar technology centre, Met Office, Beaufort Park, Easthampstead, Wokingham, RG40 3DN, UK

<sup>2</sup>Direction des Systèmes d'Observation, Météo France, 7 rue Teisserenc de Bort, BP 202, 78195 Trappes Cedex, France

**Abstract.** In radar data, the presence of untreated non-meteorological echoes has repeatedly caused severe overestimates in rainfall measurements. Improvements in the detection rate and suppression of ground clutter echoes particularly resulting from anomalous propagation of the signal (anaprop), are key issues for operational applications as concluded by COST-717 action on “Using Radar Information for Assimilation into Atmospheric Models”. Many techniques have been developed to mitigate the problem, but to date very few schemes have been reported to successfully isolate anomalous propagation returns embedded in precipitation echoes. An approach based on the difference of the signal decorrelation time between precipitation and clutter echoes has been the focus of studies conducted for several years by Météo-France and more recently by UK Met Office. Although this technique appears ineffective against sea clutter and clear air echoes, results substantiate 96–99% detection of ground fixed echoes, a level of false alarm better than 2%, and identification of anaprop echoes in situations where other techniques have failed. The amount of data processing required is minimal, ideal for operational applications. Moreover, the decorrelation time was observed to vary with the precipitation type, and in the future could serve as an additional tool for identification of snow showers.

major source of errors in rainfall measurement can be attributed to unidentified ground clutter (Holleman, 2000), particularly those generated by atmospheric super-refraction conditions causing anomalous propagation of the beam (anaprop and sea clutter). The presence of clutter echoes may produce signals reaching 60 dBZ, which is comparable with echoes observed during severe thunderstorms (Jamet et al., 1998; Sugier, 2001).

The most widely used technique for suppression of clutter echoes is the use of a clutter map (e.g. Meischner et al., 1997), which eliminates the problem of regular ground clutter but fails to identify temporary anaprop returns, and does not account for long term clutter fluctuations (e.g. seasonal growth of vegetation or installation/removal of new clutter objects; change in radar sensitivity). In the past, the Met Office has overcome the problem caused by anaprop and sea clutter with a post-processing technique based on the estimate of a probability of precipitation which relies heavily on cloud information derived from Meteosat IR and Visible imagery (Harrison et al., 2000). Over the years, this scheme has performed well according to a strict requirements of not deleting precipitation echoes, and consequently has not always successfully removed all anaprop echoes particularly under anticyclonic conditions where anaprop coincides with extensive cloud cover.

For those radar systems with Doppler capability, filtering of the radial velocity signal can suppress clutter and anaprop echoes (e.g. Seltmann and Riedl, 1999). This technique has been shown to have a level of rejection of better than 90% for clutter echo, and around 60% for anaprop (Archibald, 2000). However, this technique does not discriminate between volumes of nearly stationary rain and clutter, and exhibits difficulty in removing sea clutter echoes. Other techniques developed more specifically to tackle anaprop echoes are based on the analysis of the three-dimensional structure of the reflectivity field (Lee et al., 1995; Steiner and Smith, 2002). An elaborate neural network approach based on the characteristics of the reflectivity profile, has been developed for the Weather Surveillance Radar-1988 Doppler (WSR-88D) using volume scans collected over two years by the Tulsa, Ok-

## 1 Introduction

For several years, Météo-France and UK Met Office have been developing in-house radar processing systems, designed to optimise the entire data processing chain towards meeting changing customer requirements. These have prompted studies to develop an improved form of identification of clutter and anaprop returns.

A recent review carried out as part of the framework COST-717 action on “Using Radar Information for Assimilation into Atmospheric Models” has highlighted that a ma-

lahoma, WSR-88D (Krajewski and Vignal, 2000). However, this technique requires the careful selection of a substantial site specific training dataset, which makes this approach not readily applicable.

Wessels and Beekhuis, 1994, reported that the inherent fluctuation of meteorological signal and the relative stability of clutter signal can be used to identify clutter returns. The Royal Netherlands Meteorological Institute (KNMI) has implemented this approach operationally using the RVP-6 processor since 1996; it has exhibited an overall efficiency of more than 95% detection of clutter, and better than 2% false alarm (Wessels and Beekhuis private communication, 2002). The fluctuation of the signal is expressed as the difference of the power returns at the same range gate separated by a delay  $\tau$ :

$$\Delta_k = 10 \cdot |\log P_k - \log P_{k-\tau}| \quad (1)$$

$$Ci = \frac{1}{M-1} \cdot \sum_k^M \Delta_k \quad (2)$$

- $Ci$  (or clutter indicator) is the average signal variability in dB,
- $\Delta_k$  represents a measure of signal variability in dB (also referred to as variance),
- $P_k$  is the power of the signal at a particular range gate for a transmitted pulse  $k$ ,
- $P_{k-\tau}$  is the power of the signal at a particular range gate for a transmitted pulse  $k-\tau$ , that proceeds pulse  $k$  by a time delay  $\tau$ ,
- $M$  is the number of samples used in the calculus.

The distribution of the averaged signal variability i.e.  $Ci$  – Eq. (2) – for clutter targets is between 0 and 2 dB, whilst the spectrum for hydrometeors is typically centred around 6–7 dB (Wessels and Beekhuis, 1994; Sugier, 2001). However, the two spectra are not necessarily distinct (Fig. 1). Assuming that the stability of the transmitter is adequate, the degree of separation between clutter and precipitation spectra depends on the decorrelation time of the signal which is influenced by the nature of the target, the rotation rate of the antenna and the time delay  $\tau$ . For weather targets, the decorrelation time is also affected by a number of other factors, principally fall velocity and turbulence. Precipitation types such as snow are expected to exhibit a longer decorrelation time than convective precipitation for example, resulting in a broader spectrum extending to low  $Ci$  values (Fig. 3b). Similarly, clutter targets are not necessary homogenous, thus acting to magnify the effects of antennae rotation, and together with factors such as vegetation cover and wind, serve to broaden the spectra to high  $Ci$  values. A key issue to this approach is to define the time delay  $\tau$  necessary to best discriminate between the wide range of clutter and weather targets encountered in the British and French network.

Météo-France and the Met Office have carried out independent experiments to optimise the technique proposed by

**Table 1.** Summary of Météo-France and Met Office pre-processing parameters

	Météo-France	Met Office
Pulse length	$2 \mu\text{s}$	$2 \mu\text{s}$
Initial bin length	150 m	300 m
Scan strategy	3 elevations in 5 min 1.2°, 0.8°, 0.4°	4 elevations in 5 min 4.0°, 2.5°, 1.5°, 0.5°
Rotation rate	0.83 rpm (or 5°/s)	1.2 rpm (or 7.2°/s)
PRF	330 Hz	300 Hz
Interval between pulse	3 ms	3.3 ms
Time delay $\tau$	9 ms	6.6 ms

Wessels and Beekhuis for their respective networks. Preliminary studies have been conducted on raw data collected from various radar sites, in order to define the effects of the antenna rotation rate and of the time delay on the quality of the clutter to precipitation discrimination. Subsequently, the technique was implemented on both networks, but each country decided on different approaches. Results are presented which illustrate their respective limitations and merits.

## 2 Radar data pre-processing

### 2.1 Météo-France pre-processing chain

The mode of operation for Météo-France systems consists of scanning three elevations every 5 min, at a rotation rate of 5°/s, using a  $2 \mu\text{s}$  pulse length at 330 Hz Pulse Repetition Frequency (PRF) (summarised in Table 1). Each pulse is digitised at 1 MHz to a maximum range of 256 km giving 1700 samples per pulse at a resolution of 150 m. Following corrections of the data to compensate for the effect of the receiver characteristics and of the falling power density with range, the data are processed into instantaneous rainfall rate and signal variability values i.e.  $\Delta$  or variance – Eq. (1) – for each  $150 \text{ m} \times 0.015^\circ$  polar cell. These algorithms are implemented on a digital signal processor (DSP), connected to a VME based processing system (CASTOR) running Vx-Works. Finally, the averaging process takes place during conversion to the  $1 \text{ km} \times 1 \text{ km}$  Cartesian format, and during the production of a  $1 \text{ km} \times 1^\circ$  polar product (Lamarque, 2002).

### 2.2 Met Office pre-processing chain

The mode of operation for Met Office systems is to scan four elevations every 5 min, at a rotation rate of 7.2°/s, using a  $2 \mu\text{s}$  pulse length at 300 Hz PRF (summarised in Table 1). Each pulse is digitised at 500 kHz to a maximum range of 255 km, giving 850 samples per pulse at a resolution

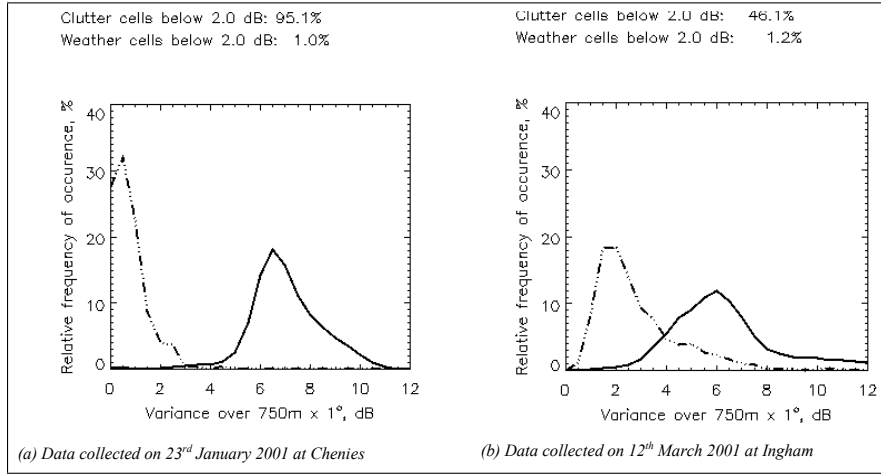


**Fig. 1.** Distribution of the signal fluctuation at  $750 \text{ m} \times 1^\circ$  resolution versus frequency of occurrence, for precipitation echoes (solid line), and for clutter echoes (dashed line). Pixels with clutter echoes were selected during dry condition from pixels with high frequency of detection, i.e. pixels detected more than 90% of the time. Conversely, pixels with precipitation echoes were selected from pixels with a low frequency of detection (i.e. pixels detected less than 10% of the time).

of 300 m as input to the DSP. Sampled amplitudes are in the form of raw digital counts at 12-bit resolution (i.e. 72 dB dynamic resolution), which are first converted into square root of power and adjusted for linearisation and for receiver characteristics. The output from the DSP is in the form of averaged reflectivity and  $C_i$  values – Eq. (2) – for each  $750 \text{ m} \times 1^\circ$  polar cell, and is fed into a PC based processing system (CYCLOPS). The main functions of Cyclops consist of controlling the radar operation, and pre-processing the data to allow the dissemination of raw polar data to the central processor.

### 3 Identification of targets

Figure 1 shows the distributions of  $C_i$  values for clutter and for meteorological echoes, derived from data collected at two UK radar sites (at Chenies near London; and at Ingham in the east of England). These results substantiate a clear separation between clutter and precipitation spectra.

At both locations, only a small fraction of rain pixels (around 1%), has a  $C_i$  value below 2 dB. During dry conditions, 95% of  $C_i$  values are observed to be below 2 dB at Chenies, whereas the figure is only 46% at Ingham. Hence, the decorrelation time for clutter signals is shorter at Ingham than that observed at Chenies, due to the different nature of the surrounding clutter. At Chenies, clutter echoes are mostly produced by stable structural returns from urban constructions, whereas at Ingham clutter echoes are generated from vast farming fields prone to be affected by the wind.

The effect of the antenna rotation rate on the signal decorrelation time is illustrated in Fig. 2. The mode of the distribution of  $C_i$  for precipitation echoes varies between 5.5 dB for a large time delay between samples of 12 ms at  $5^\circ/\text{s}$ , to 4.5 dB for a delay of 4 ms at  $10^\circ/\text{s}$  and  $15^\circ/\text{s}$ . The mode of the distribution for clutter echoes is close to 0.8 dB for a short time delay of 4 ms at  $10^\circ/\text{s}$ , increasing to 1.5 dB for 8 ms at  $15^\circ/\text{s}$ . For each set of time delays (4 ms and 8 ms), the change in rotation rate (from  $10^\circ/\text{s}$  to  $15^\circ/\text{s}$ ) does not appear to have

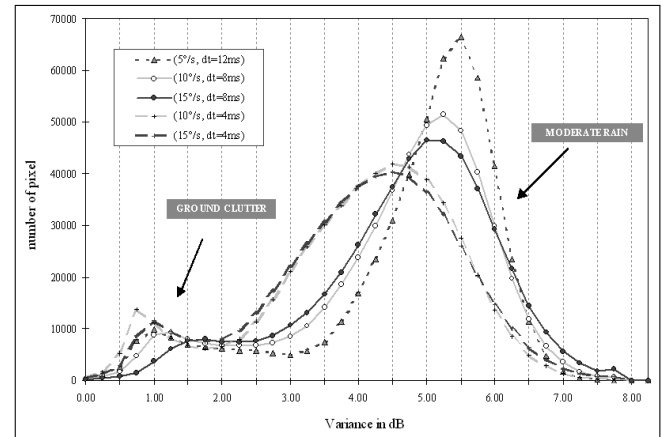


**Fig. 2.** Distributions of the signal variability for various rotating speed and different time lag. Data below the noise threshold are removed from the analysis. Data collected at the Bollène radar site, in the Rhône Vallée, and processed by ALICIME for Météo-France, at a resolution of  $1 \text{ km} \times 1 \text{ km}$ .

an effect on the distribution for precipitation echoes, whereas for clutter returns these changes appear to shift the mode of the distribution by up to 0.5 dB. Furthermore, for an increase of the pulse interval from 4 ms to 12 ms the mode of the distribution for precipitation echoes increases by around 1.0 dB, while the standard deviation reduces. Thus, this experiment shows that the separation between clutter and precipitation is better achieved with a larger time delay, and with a slow rotation rate.

At a fixed pulse interval of 6.6 ms, and a rotation rate of 1.2 rpm, the separation between clutter and precipitation  $C_i$  distributions varies with precipitation types. Snowflakes are found to produce a broader distribution of  $C_i$  values (Fig. 3b) by comparison with hail (Fig. 3f) or rain returns (Fig. 1). This information might serve as an additional parameter to help in distinguishing for example between snow and rain.

Further examination of Fig. 3 shows that for all types of return the proportion of  $C_i$  values below 2 dB decreases with

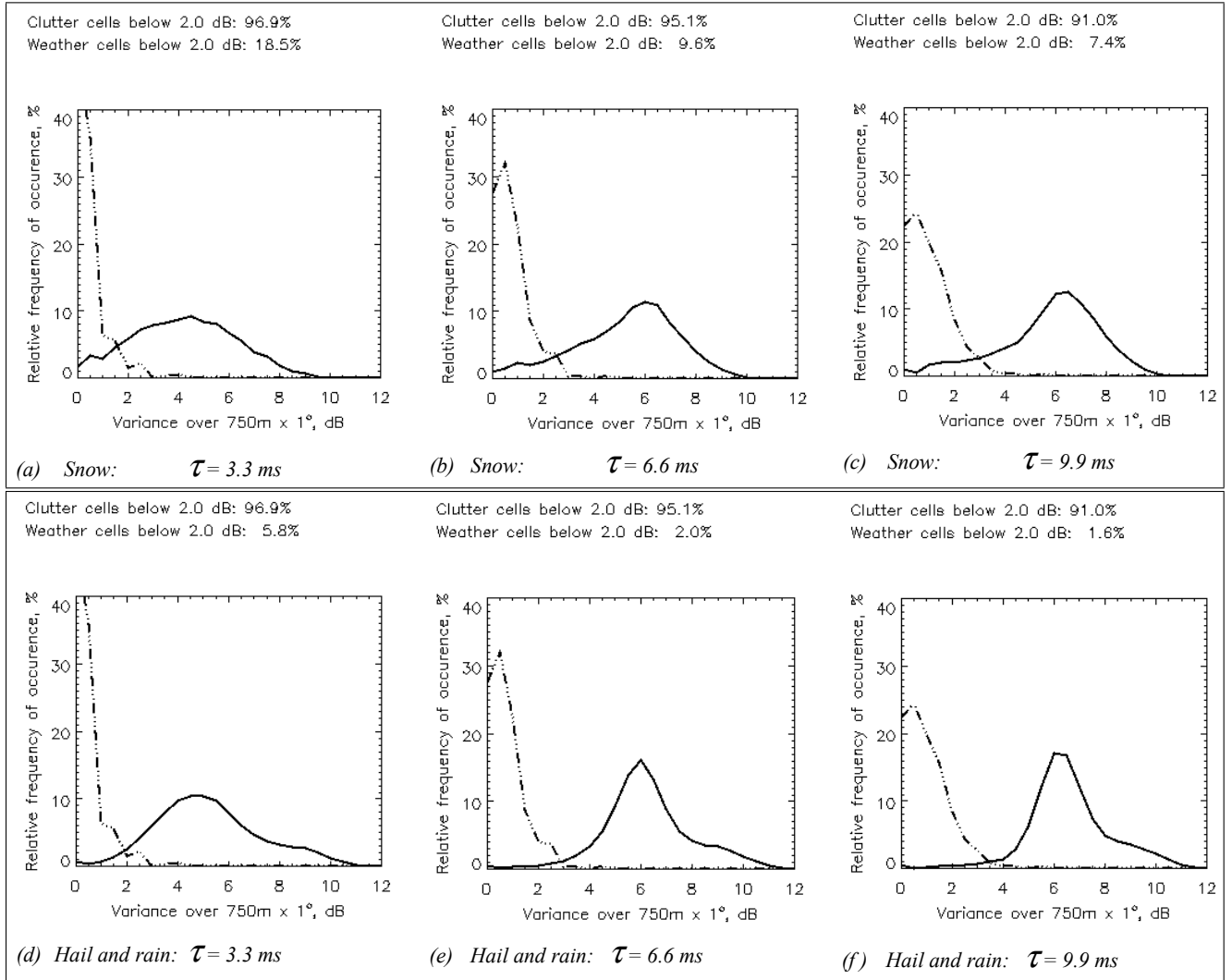


**Fig. 3.** Distribution of the signal fluctuation at  $750\text{ m} \times 1^\circ$  resolution, for precipitation echoes (solid line), and for clutter echoes (dashed line), for various time delays. Snow data ((a), (b), (c)) were collected on 19 January 2001, and a mixture of hail and rain data ((d), (e), (f)) were collected on 26 January 2001, at the Chenies radar site (NW of London).

increasing time delay  $\tau$  (Fig. 3). At 9.9 ms signals from clutter echoes are on the verge of being decorrelated (i.e. producing  $C_i$  values similar to those found for rain), while the distribution for precipitation does not significantly vary between 6.6 ms and 9.9 ms (Fig. 3). Thus at 1.2 rpm, discrimination between all types of precipitation and clutter is best achieved using a time delay of 6.6 ms.

## 4 Operational implementation

Météo-France and the Met Office decided on different approaches for implementation of the technique.

### 4.1 Météo-France scheme

Météo-France chose to implement within the DSP a filter based on the variance value ( $\Delta k$  – Eq. (1)), at a resolution of  $150\text{ m} \times 0.015^\circ$ . A fixed attenuation of 30 dB is applied

to cells with a  $\Delta k$  value of 2 dB or less. For cells with a  $\Delta k$  value between 2 and 3.5 dB, an attenuation of 20 dB/dB is used. This method has been used for several years on the French operational network, and has received positive feedback from meteorologists. However it has also given rise to problems for hydrological applications because of possible irreversible damage to genuine precipitation echoes.

Following recent studies, the scheme has been revised to simultaneously provide products with and without clutter filtering along with a variance product. Furthermore, the time delay was increased from 3 ms to 9 ms (at 0.83 rpm) and has resulted in the reduction of false alarm to less than 2%.

### 4.2 Met Office scheme

Rather than explicitly correcting the reflectivity estimate, Met Office chose to adopt a multi-step rejection-based approach. This makes the occurrence of false alarms manageable, and provides a more flexible framework for responding

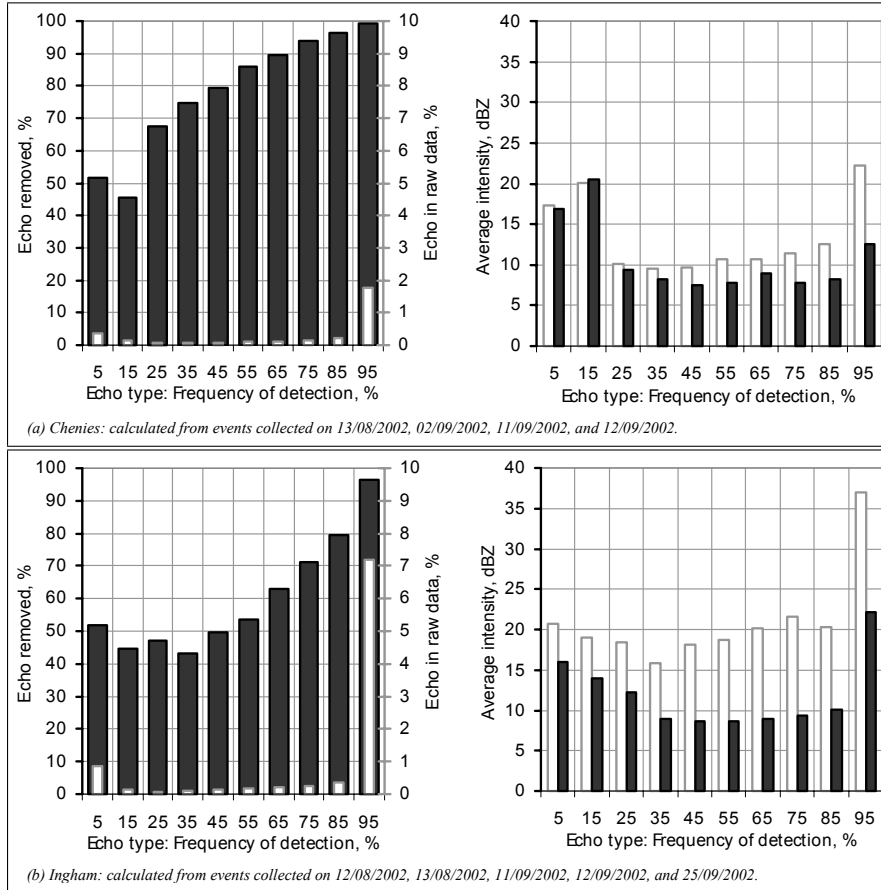


**Fig. 4.** Quality description of the clutter suppression scheme by analysis of data collected during dry weather events at two contrasting radar sites. Diagrams on the left show the percentage of echoes present in the raw data product (white), and percentage of echoes removed by the scheme (black). Diagrams on the right give the average intensity of the echoes before (white) and after (black) having applied the clutter removal scheme.

to changing conditions. Although, this procedure has not yet been operationally implemented on the UK network, it has been successfully tested on numerous events in parallel with the current operational system. The new scheme has required changes to the processing chain, and was designed to operate on a newly developed central processing system (RADAR-NET4), which is taking over major tasks currently performed at the radar site by Cyclops.

The Met Office clutter removal scheme proceeds in three stages:

- The first step removes all polar pixels with a  $C_i$  value below 2 dB, which represents the removal of 45–95% of clutter cells. This step may be by-passed in the event of high probability of snow, based on precipitation types report.
- The objective of the second step is to deal with the overlapping region of clutter and precipitation  $C_i$  distributions, i.e. for pixels with a  $C_i$  value between 2 and 3.5 dB. To suppress the blind removal of precipitation with marginal signal variability, a dynamic clutter map is used to remove pixels classed as (usually) cluttered AND with a  $C_i$  value below 3.5 dB.
- Subsequently the picture is cleared of isolated pixels with a speckle filter.

The site-specific dynamic clutter map is produced centrally every month, based on the three-monthly accumulative detection of echoes above noise threshold (around 3 dBZ at close range, and 1 dBZ at 255 km). The map is expressed in percent and in terms of frequency/probability of detection (POD).

## 5 Case studies

### 5.1 Method of evaluation

Because there is no accessible independent method of identifying clutter, anaprop, or precipitation echoes, it is almost impossible to quantify the quality of a clutter suppression scheme, particularly for those cases where weather and clutter echoes occur in the same pixel. Comparison of radar and rain gauge data could serve to identify the occurrence of false alarms, however this procedure would have to be very costly to be effective.

As part of the OPERA consortium, Holleman et al. (2002), produced guidelines for exchanging a quality product between Met. Services. For the purpose of harmonising the assessment of the wide range of clutter removal schemes employed across Europe, Holleman et al. (2002), proposes the quantification of the number of clutter contaminated pix-

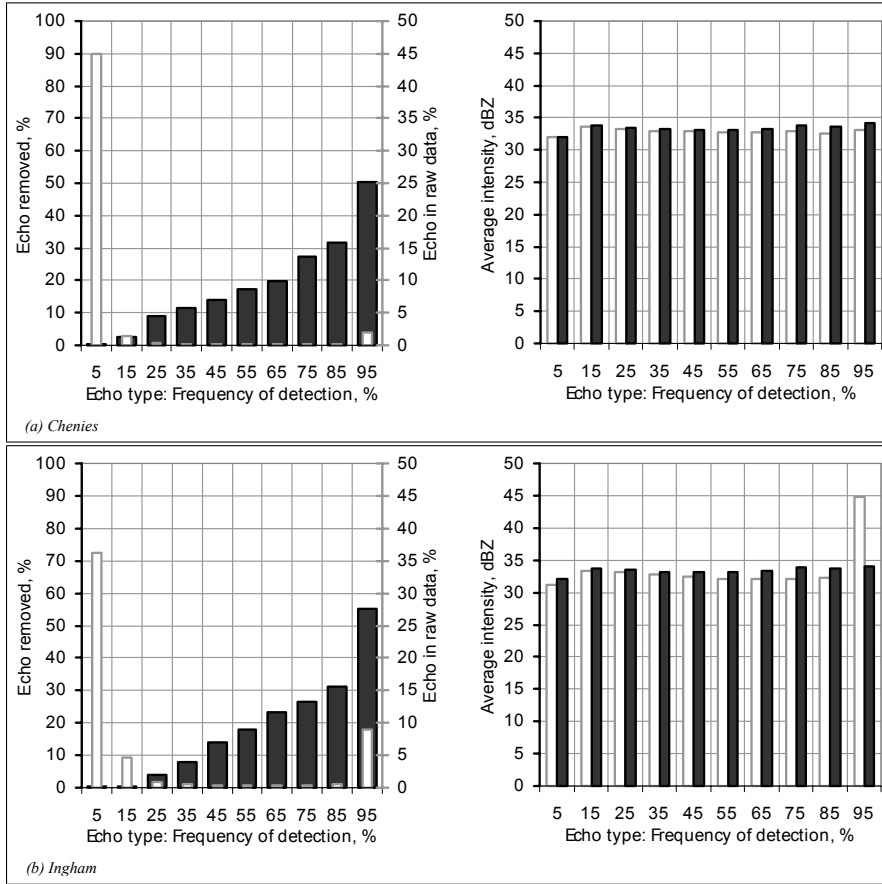


**Fig. 5.** Quality description of the clutter suppression scheme by analysis of data collected during a slow moving frontal event (9 September 2002). Diagrams on the left show the percentage of echoes present in the raw data product (white), and percentage of echoes removed by the scheme (black). Diagrams on the right give the average intensity of the echoes before (white) and after (black) having applied the clutter removal scheme.

els present in the product image, and of the mean value of the intensity of all clutter contaminated pixels. Additionally as part of this work, the echo type may be classified using a three-monthly POD, for which ground fix echoes have a POD above 90% and rain echoes have a POD below 10%. Thus, the performance of the clutter removal process may be expressed in terms of the percentage of pixels removed with POD greater than 90%, under dry condition. Similarly the percentage of precipitation wrongly deleted may be estimated in terms of the percentage of pixels removed with POD less than 10%, under wet condition.

## 5.2 Dry weather events

The quality of the clutter suppression scheme under dry conditions is shown in Fig. 4. It illustrates the efficiency of the removal scheme for scans believed to be composed entirely of ground fixed clutter returns (i.e. no anaprop). A POD is associated with each return, based on the site-specific dynamic clutter map, and serves to illustrate that more than 96% of fixed clutter targets (i.e.  $\text{POD} > 90\%$ ), are successfully removed by the scheme. Therefore, this technique also removes clutter returns with a lesser frequency of detection, which would have been overlooked by a traditional static clutter map

## 5.3 Wide spread frontal event

The quality of the clutter suppression scheme under wet conditions is shown in Fig. 5. It illustrates the efficiency of the removal scheme for scans believed to be composed merely of ground fixed clutter and rain returns (i.e. no anaprop). A POD is associated with each return based on the site-specific dynamic clutter map, and serves to illustrate that less than 1% of rain pixels (i.e.  $\text{POD} < 10\%$ ), are removed by the scheme.

## 5.4 Anaprop echoes near and embedded in precipitation

Visual examples of the effectiveness of Met Office and Météo-France schemes to detect anaprop echoes embedded in rain are shown in Figs. 6 and 7. The  $C_i$  products for such events are presented in Fig. 6, while Fig. 7 shows two examples of accumulation products before and after clutter suppression. (Note that these examples are best viewed in colour, and can be downloaded from <http://www.copernicus.org/erad/>).

## 6 Conclusions

Météo-France and Met Office have carried out independent studies regarding the implementation and benefits of a clutter suppression technique based on statistical analyses of signal fluctuation. For meteorological returns, the decorrelation

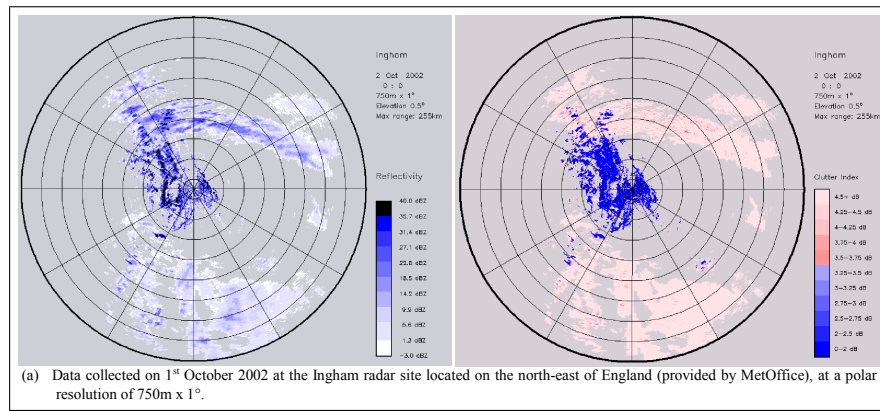


**Fig. 6.** Untreated reflectivities (left) and  $Ci$  products (right). The images are comprised of a mixture of precipitation, clutter and anaprop echoes, not evidently distinguished from the reflectivity image alone (left). However, all becomes apparent with the variance products (right) which reveal rain (high variance), and ground clutter and anaprop variance (low variance).

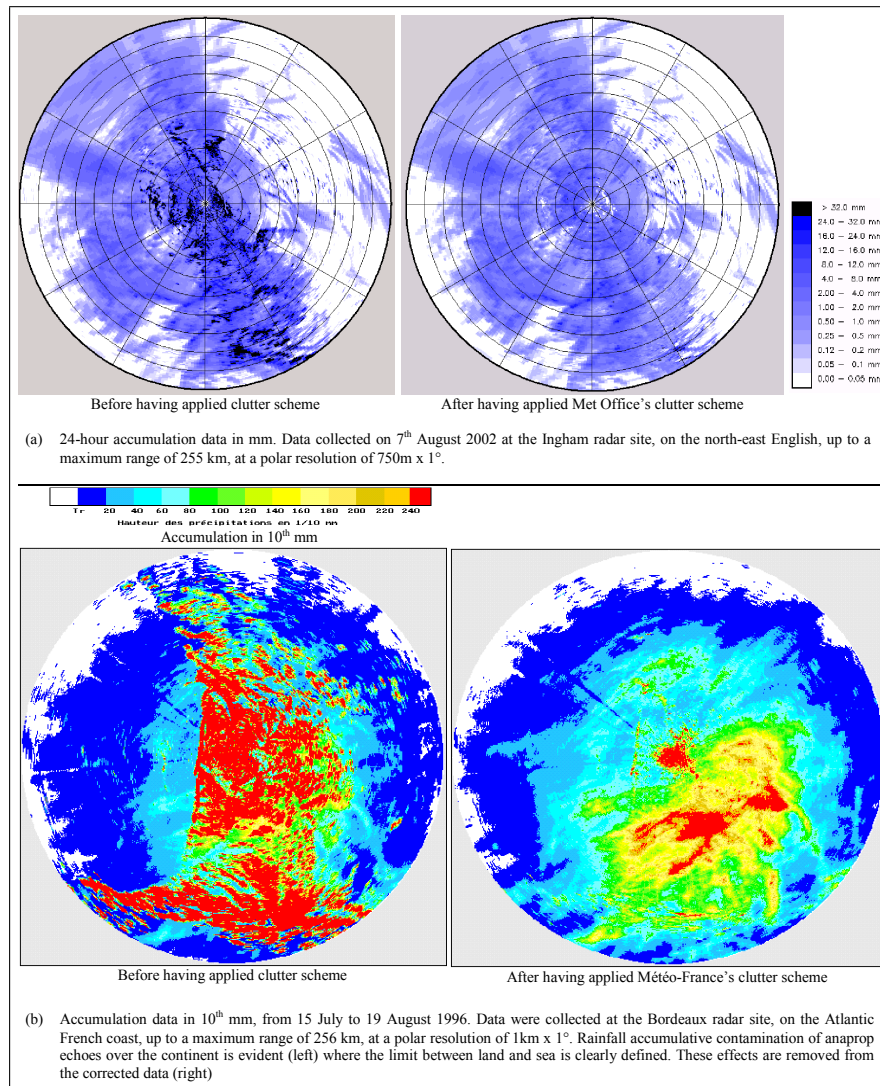


**Fig. 7.** Untreated accumulation data (left) and treated accumulation data (right). The images are comprised of a mixture of precipitation, clutter and anaprop echoes, the latter giving rise to high accumulation values in the untreated picture (left), which are removed (Met Office's scheme) or attenuated (Météo-France's scheme) in the treated picture (right).

time decreases with increasing time interval between pulses but does not exhibit sensitivity to change in the antenna rotation rate. Conversely for clutter targets, the decorrelation time is mostly influenced by the antenna rotation rate.

Operational implementation and parallel testing of the technique have been carried on both networks. The improved clutter suppression scheme requires little processing power and can be implemented with a high degree of flexibility to suit individual network requirements and implementation platforms. Results have demonstrated the particular effectiveness of this technique in detecting anaprop embedded in rain. As far as can be determined, the scheme appears to successfully retain precipitation echoes in closely combined clutter/rain areas.

*Acknowledgement.* The authors would like to thank Ewan Archibald and Herman Wessels for helpful discussions, and George Ball for providing expertise on technical aspects of operational implementation.

## References

- Archibald E.: Enhance Clutter Processing for the UK Weather Radar Network. *Phys. Chem. Earth*, 25, 823–828, 2000.
- Harrison, D. L., Driscoll, S. J., and Kitchen, M.: Improving precipitation estimates from weather radar using quality control and correction techniques. *Meteorological Applications*, 6, 135–144, 2000.
- Holleman I.: Processing of radar reflectivity data – a review. Working document number WDD\_03\_200009\_1, <http://pub.smhi.se/cost717/>, 2000.
- Holleman, I., Galli, G., and Urban, B.: Definition of product quality descriptors. Working document number WD\_05\_02, OPERA project 1c3, 2002.
- Jamet G., Roquain, P., and Pugliese, P.: Radar de Bordeaux – Résultats de la campagne de test sur l'éliminateur d'échos fixes Thomson. Rapport d'essai Météo-France DSO N° S011, 1998.
- Krajewski, W. F. and Vignal, B.: Evaluation of anomalous propagation echo detection in WSR-88D data: A large sample case study. *American Meteorological Society*, 807–814, 2001.
- Lamarque, P.: Comparaison des calculateurs CASTOR et CASTOR2 sur le radar de Trappes. Rapport d'essai Météo-France DSO, N° S030, 2002.
- Lee, R., Bruna, G. D., and Joss, J.: Intensity of ground clutter and of echoes of anomalous propagation and its elimination. 27th conference on Radar Meteorology, *American Meteorological Society*, 651–652, 1995.
- Meischner, P., Collier, C., Illingworth, A., Joss, J., and Randeu, W.: Advanced weather radar systems in Europe: The COST 75 Action. *Bulletin of the American Meteorological Society*, 78, 1411–1430, 1997.
- Perier, L.: Radar de Précipitation : Test sur la discrimination entre échos de sol et échos de précipitation. Rapport d'essai Météo-France DSO N° S019, 2000.
- Seltmann, J.E.E. and Riedl, J.: Improved clutter treatment within the German radar network: First results. COST 75 Advanced Radar Systems, International Seminar, Locarno. European Commission, 267–279, 1999.
- Steiner, M. and Smith, J. A.: Use of three-dimensional reflectivity structure for automated detection and removal of non-precipitating echoes in radar data. *American Meteorological Society*, 673–686, 2002.
- Sugier, J.: A reviewed signal processing scheme for Met Office radar systems. Technical report No. 36, Met Office, 2001.
- Wessels, H. and Beekhuis, J.: A stepwise procedure for suppression of anomalous ground clutter echoes. COST 75 Weather Radar Systems International Seminar, Brussels, Belgium. European Commission (EUR 16013 EN), 270–277, 1994.